Journal of Biomedical Optics

SPIEDigitalLibrary.org/jbo

Detection of brain tumors using fluorescence diffuse optical tomography and nanoparticles as contrast agents

Pierre-Yves Fortin
Coralie Genevois
Anne Koenig
Emilie Heinrich
Isabelle Texier
Franck Couillaud

SPIE

Detection of brain tumors using fluorescence diffuse optical tomography and nanoparticles as contrast agents

Pierre-Yves Fortin,[a,b] Coralie Genevois,[a,b] Anne Koenig,[c] Emilie Heinrich,[c] Isabelle Texier,[c] and Franck Couillaud[a,d]
[a]Université Bordeaux Segalen, Laboratoire IMF, CNRS/UMR 5231, Université Bordeaux 2, France
[b]Université Bordeaux Segalen, Institut de BioImagerie, CNRS/UMS 3428, Université Bordeaux 2, France
[c]CEA/LETI Minatec, Grenoble, France
[d]Université Bordeaux Segalen, Laboratoire RMSB, CNRS/UMR 5536, Université Bordeaux 2, France

Abstract. Near-infrared fluorescence-enhanced diffuse optical tomography (fDOT) is used to localize tumors in mice using fluorescent nanoparticles as a blood pool contrast agent. The infrared dye DiR is loaded in the lipid core of nontargeted nanoparticles (DiR-lipidots) and injected systemically *via* the tail vein in mice bearing U87 tumors. Distribution and time-course of DiR-lipidots are followed using *in vivo* fluorescence reflectance imaging and reveal enhanced fluorescent signal within the subcutaneous tumors up to seven days due to the enhanced permeability and retention effect. Tumor growth into the brain is followed using bioluminescent imaging, and tumor localization is further determined by magnetic resonance imaging. The fDOT provides three-dimensional fluorescent maps that allow for consistent localization for both subcutaneous and brain tumors. [DOI: 10.1117/1.JBO.17.12.126004]

Keywords: tomography; bioluminescence; fluorescence; magnetic resonance imaging; cancer imaging; nanoparticles.

Paper 12335 received Jun. 1, 2012; revised manuscript received Oct. 29, 2012; accepted for publication Oct. 30, 2012; published online Dec. 3, 2012.

1 Introduction

Localization of tumors remains a challenge in cancer both in clinic and for preclinical models. Imaging modalities such as magnetic resonance imaging (MRI), x-ray, and ultrasound allow for detection of tumors without contrast agents. However, the use of exogenous contrast media brings dramatic improvement in the sensitivity of detection and delineation of pathological structures. In solid tumors, the enhanced permeability and retention (EPR) effect leads to the accumulation of the intravenously injected contrast material in the extra vascular space, leading to imaging signal enhancement.

For preclinical mouse model, optical imaging techniques are becoming widely used.[1] Bioluminescence imaging (BLI) is highly sensitive but requires experimental genetic engineering of cancer cells and thus is irrelevant to detect wild type tumors. By using exogenous fluorescent probes, fluorescence imaging can be used to localize tumors. Fluorescence reflectance imaging (FRI) is a two-dimensional (2-D) technique impairing precise localization of deep tumors due to photon absorption and scattering. Near-infrared fluorescence-based tomography techniques such as Fluorescence Molecular Tomography (FMT®) or fluorescence-enhanced diffuse optical tomography (fDOT) allow for the localization of deep tumors in mice.[2] The fDOT instruments operate in a trans-illumination excitation mode[3] and are assisted by sophisticated reconstruction algorithms[4] allowing reconstruction and quantification of a fluorescent signal within a mice. A fDOT imaging system was recently developed and subsequently validated with combined PET.[5] It was already used to follow tumor development in mouse lung, using a multimerized peptide RGD fluorescent probe, targeting $\alpha v\beta 3$ integrins.[6]

With this system, two types of acquisition are possible: either a constrained mode with mice compressed between two transparent plates or a free space mode. Despite the great advantage of targeted probes, unspecific fluorescent probes have been shown to be efficient for routine localization of wild type tumors based on changes in surrounding vasculature and on a so-called enhanced permeability and retention (EPR) effect.[7] This effect is related to accumulation and retention of the fluorescent probe in the extra-vascular space resulting in a fluorescent contrast. In the present paper, the combined use of the fDOT system and a nonspecific fluorescent tracer was evaluated for detection and localization of brain tumor in mice. The contrast agent used is a dispersion of lipid nanoparticles (soybean oil and Suppocire® NC core) coated by a surfactant shell made of phospholipids and poly(oxyethylene) polymers (lipidots), and loaded with a near-infrared fluorophore (DiR).[8–10] Tumor growth was followed by BLI and localized by multimodal MRI/fDOT imaging.

2 Materials and Methods

2.1 *Mouse Handling and Surgical Procedure*

Experiments were conducted in agreement with the European Commission guidelines and directives of the French Research Ministry at University Bordeaux Segalen animal's facilities. Adult female nude immuno-deficient mice (Swiss Nude, Charles River, laboratories, Lyon, France) were used in this study. For subcutaneous tumor implantation, U87-CMV-lucF cells (2×10^6 cells/100 μL) were injected on the right posterior leg. For brain tumor implantation, mice (20 to 25 g) were anesthetized

Address all correspondenc to: Franck Couillaud, Université Bordeaux Segalen, Laboratoire IMF, CNRS/UMR 5231, Université Bordeaux 2, France. Tel: (33)5 5757 4750; E-mail: franck.couillaud@u-bordeaux2.fr

0091-3286/2012/$25.00

with isoflurane (2% in air, Belamont, Nicholas Piramal Limited, London United Kingdom) and placed into a stereotaxic frame support. U87-CMV-lucF tumor cells ($6 \times 10^5/5\ \mu$L) were implanted in the brain, 1.5 mm posterior and 2.5 mm lateral to the bregma, 2.5 mm depth from the skull surface.

U87-CMV-lucF was obtained as follows. U87 human glioma cell line was obtained from the American Tissue Culture Collection (ATCC, Manassas, Virginia). Cells were maintained in DMEM (Invitrogen, Carlsbad, California) supplemented with 10% fetal bovine serum. To generate a bioluminescent glioma cell line, U87 cells were first genetically modified for random integration of FRT sites within the genome. A recombinant clone containing several FRT sites was first selected with zeocin and several insertion sites were detected by Southern blot. Then, the U87-FRT line was co-transfected with a pcDNA5-FRT plasmid containing the lucF reporter gene under the control of the constitutive CMV promoter and the pOG44 plasmid encoding for the Flp recombinase and cells were selected with hygromycin (Flp-in system, Invitrogen, Carlsbad, California). The resulting stably transformed cell line U87-CMV-lucF has been amplified and used for all implantations in nude immunodeficient mice.

2.2 *Nanoparticles Synthesis*

For the preparation of a 2 mL dispersion batch of DiR-loaded lipidots, 150 mg of Suppocire® NB (Gatefosse, France), 50 mg of soybean oil (Croda, France), 138 mg of *L-α* lecithin (Lipoïd-S75™, Germany), and 800 nmol of DiR (766 μg) (Invitrogen, France) are dissolved in 1 mL of dichloromethane and mixed at 50°C.[9] After homogenization, the organic solvent is evaporated under reduced pressure, and the lipid phase is crudely mixed with the continuous phase composed of 228 mg of Mirj® 53 (Croda, France), 50 mg of glycerol (Sigma-Aldrich, France) and 1.38 mL of 154 mM NaCl. An oil-in-water nanoemulsion is obtained by ultrasonication of the oil and aqueous phases (VCX750 Ultrasonic processor, 5 min sonication at 25% power). To separate any dye or other compounds not associated with the lipid nanoparticles, lipidots are dialyzed overnight in a large volume ($\approx$ 800 mL) of NaCl 154 mM, at room temperature and protected from the light. Samples are sterilized on 0.22 μm filters (Millipore, France), then diluted to the desired concentration, suitable for characterization and *in vivo* injection. Particle size, polydispersity, and zeta potential are characterized by dynamic light scattering (Zeta Sizer Nano ZS, Malvern Instrument). Absorbance and fluorescence spectra, respectively measured with a Cary 300 scan ultraviolet (UV)-visible spectrophotometer (Varian) and a Perkin-Elmer LS50B fluorimeter, allow the optical characterization of the particles as well as the quantification of dye-loading. Lipid nanodroplets are obtained at a concentration of 4.5×10^{15} particles/mL. They exhibited a diameter of 37 ± 2 nm, a polydispersity index of 0.12 ± 0.02, and a zeta potential of -2.5 ± 2.0 mV. A mean value of 9 DiR fluorophores per particle core is calculated based on absorbance spectra (180 μM dye, 90% encapsulation yield, absorption maximum 750 nm; emission maximum 770 nm).

2.3 *In Vivo Bioluminescence Imaging*

Bioluminescence images of mice were acquired using a NightOWL II LB 983 system equipped with a NC 100 deep-cooled (−70°C) CCD camera (Berthold Technologies, Bad Wildbad, Germany). Mice were injected intra-peritoneal with D-luciferin [Promega, Madison, Wisconsin, 2.9 mg in 100 μL sterile phosphate buffer (PBS)] and were sedated 5 min later with isoflurane (2% in air). Bioluminescence images (2 min integration periods, 4×4 binning) and photos (100 ms exposition) were taken 8 min after the luciferin injection on anesthetized mice. A low light-emitting standard (Glowell, LUX biotechnology, United Kingdom) was placed next to the animal during each image acquisition to provide a constant reference for the resulting images. Grayscale body-surface reference images were collected for superposition of BLI images on anatomical maps. Pseudocolor luminescent images representing the spatial distribution of emitted photons were generated using IndiGO™ 2 software (Berthold Technologies, Bad Wildbad, Germany). BLI analysis was done semi-automatically by first placing a small region of interest (ROI). Within this ROI, the mean light intensity (Photons $\cdot$ s^{-1} $\cdot$ mm^{-2}) was measured.

2.4 *Fluorescent Diffuse Optical Tomography*

Mice were injected intravenously with 200 μL of lipid nanoparticle suspension in PBS isotonic to blood (100 μM DiR; 5×10^{14} particles). Before and at different times after injection, mice were anesthetized (2% isoflurane in air) and positioned on a dedicated holder. For brain tumor detection, mouse head is gently maintained between the bottom glass plates, and a small, upper glass plate positioned on the mouse head. For a subcutaneous tumor, the free space mode was used.[11] The holder is placed in the dark chamber of the fDOT prototype. The instrument consists of a laser source (690 nm, 21 mW, Powertechnology) mounted on two motorized translation stages and a CCD cooling (−30°C) camera (Hamamatsu Orca AG, Massy, France). The laser is placed under the animal for transillumination. Typically, the excitation source describes a regular 11×11, 2 mm spaced grid (2×2 cm^2 field of view) under the examined sample. For each source position, the CCD camera focused onto the upper glass window, records at first the transmitted (excitation) images. Then a RG9 high-pass filter (cut off at 720 nm, Schott, Mainz, Germany) is inserted, and the fluorescence (emission) images are acquired. The exposure time is adapted for each source position in order to take advantage of the entire dynamic range of the camera, even in highly heterogeneous regions of the animal. The transmitted images lead to the reconstruction of an optical heterogeneity map; it depicts compounds of the intrinsic tissues heterogeneity and the border effects due to the complex shape of the turbid medium.

The second step is the reconstruction of the fluorescence yield from the fluorescent images using this heterogeneity map. Convergence of the algorithm is achieved within 15 iterations by using a classical iterative ART algorithm with a relaxation parameter of 0.1.[12]

2.5 *Fluorescence Reflectance Imaging (2D-FRI)*

The fDOT prototype could also be used for FRI using a light emitting diode (LED) ring at 660 nm (Hamamatsu) as excitation source. Near-infrared fluorescence images (exposure time 1 s) were acquired through the RG9 filter by the charge coupled device (CCD) camera.

2.6 *Magnetic Resonance Imaging*

Animals were sedated with isoflurane (2% in air) and maintained in the fDOT double plate holder. The animal was

positioned in prone position into the MRI scanner (1.5 Tesla, Achieva Philips Healthcare). A 23-mm surface receiver coil was positioned above the head mouse hind leg to provide sufficient signal-to-noise ratio.T1-weighted (TR/TE = 650/7.6 ms) and T2-weighted (TR/TE = 2220/80 ms) sequences were performed in coronal view, with a 0.31 mm in plane resolution, to localize and to measure the size of the tumors. Slice thickness of both, MR and reconstructed three-dimensional (3-D) fluorescent images, were identical (1 mm).

3 Results

3.1 *Time Course of DiR-Lipidots Fluorescence in Mouse-Bearing Subcutaneous Tumor*

U87-CMV-lucF cells were injected to generate subcutaneous tumors in immuno-deficient mice ($n = 6$). Tumors were left growing for about two months, taking care that diameter never exceeded 10 mm. Tumors were then assayed for lucF expression by BLI to attest the presence of viable U87-CMV-lucF cells within the tumor [Fig. 1(a)]. Mice were quickly transferred from BLI system to fDOT machine and mice autofluorescence was determined by 2D-FRI [Fig. 1(b)] and fDOT using the free space mode [Fig. 1(g)]. The 3-D fluorescent maps computed using the fDOT software provide a stack of 18 fluorescent slices with 1 mm of thickness, from ventral ($z = 0$) to dorsal ($z = 17$). As shown on Fig. 1(g), no fluorescent signal was found within the 3-D reconstruction maps.

Mice are allowed to wake up from isoflurane anesthesia and 10 min later injected intravenously by 200 μL of DiR-lipidots solution. As shown on Fig. 1(c) and 1(d), the fluorescence level as determined by 2D-FRI, rapidly increases in the whole body of the animal and in the tumor. A maximum of fluorescence was observed 4 h after injection, and then 2D-FRI signal slowly decreased [Fig. 1(f)]. The fluorescence level in the ROI located on the subcutaneous tumors was more intense and decreased more slowly than in ROIs placed on other areas of the mouse [Fig. 1(e)]. The difference in fluorescence levels between inside and outside the tumor was maximum 8 h post-injection, [Fig. 1(f)]. The fluorescent signal of DiR fluorophore remained detected in the tumor up to seven days after injection. A fDOT acquisition was performed 24 h post-injection [Fig. 1(h)] using the free space mode with 3-D reconstruction maps. The signal of fluorescence found on slices $z = 9$ to $z = 13$ was consistent with an accumulation of DiR fluorophore into the tumor.

3.2 *Multimodal Detection of Brain Tumors Using BLI/fDOT/MRI*

After stereotaxic injection of U87-CMV-lucF cells into the brain (right parietal area), tumor growth was followed every week by BLI. The BLI signal was used to determine the optimal time for DiR-lipidots injection. Small tumors exhibiting BLI signal lower than 50,000 photons $\cdot$ s^{-1} $\cdot$ mm^{-2} were found not detectable using fDOT and the current MRI setup (data not shown).

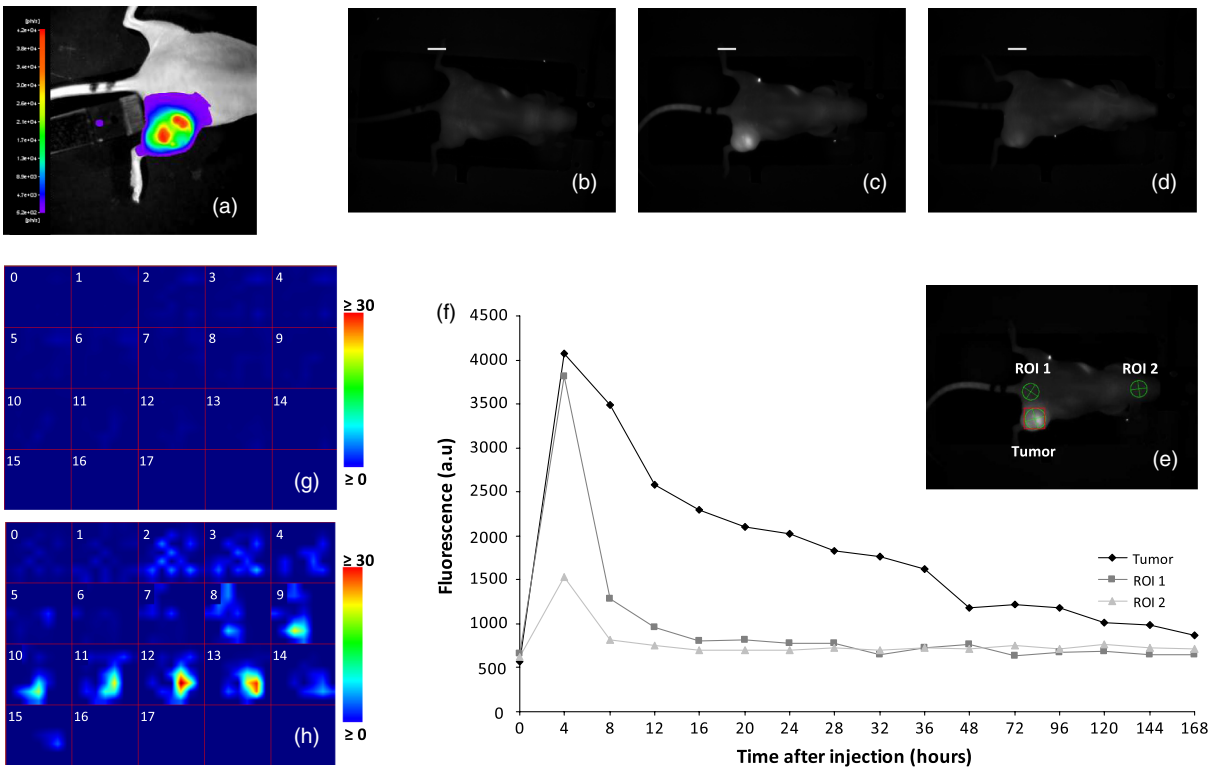

Fig. 1 Optical imaging of a subcutaneous tumor. (a) Bioluminescence image of a mouse bearing a U87-CMV-lucF tumor. Next to the mouse, a low light-emitting standard is placed. (b), (c), (d) fluorescence reflectance imaging of the same mouse before (b); 24 h (c), and 120 h (d) after systemic injection of DiR-lipidots. White bar represents 9 mm (e) position of regions of interest (ROI) for quantification by FRI (circle). Square represents the scanning zone for fDOT. (f) Evolution of the fluorescent level after DiR-lipidots intravenous injection in the 3 different ROI (ROI 1 is an area on the back of the mouse; ROI 2 is on the head and ROI 3 is on the subcutaneous tumor as illustrated in panel E). (g) and (h): Results of fDOT reconstructions before (g) and 24 h after (h) DiR-lipidots injection. Z cross-sections (1 mm thickness) are presented in the same color scale from $z = 0$ (ventral) to $z = 17$ (dorsal). fDOT images were acquired using the free space mode. Images are representative of $n =$ six mice.

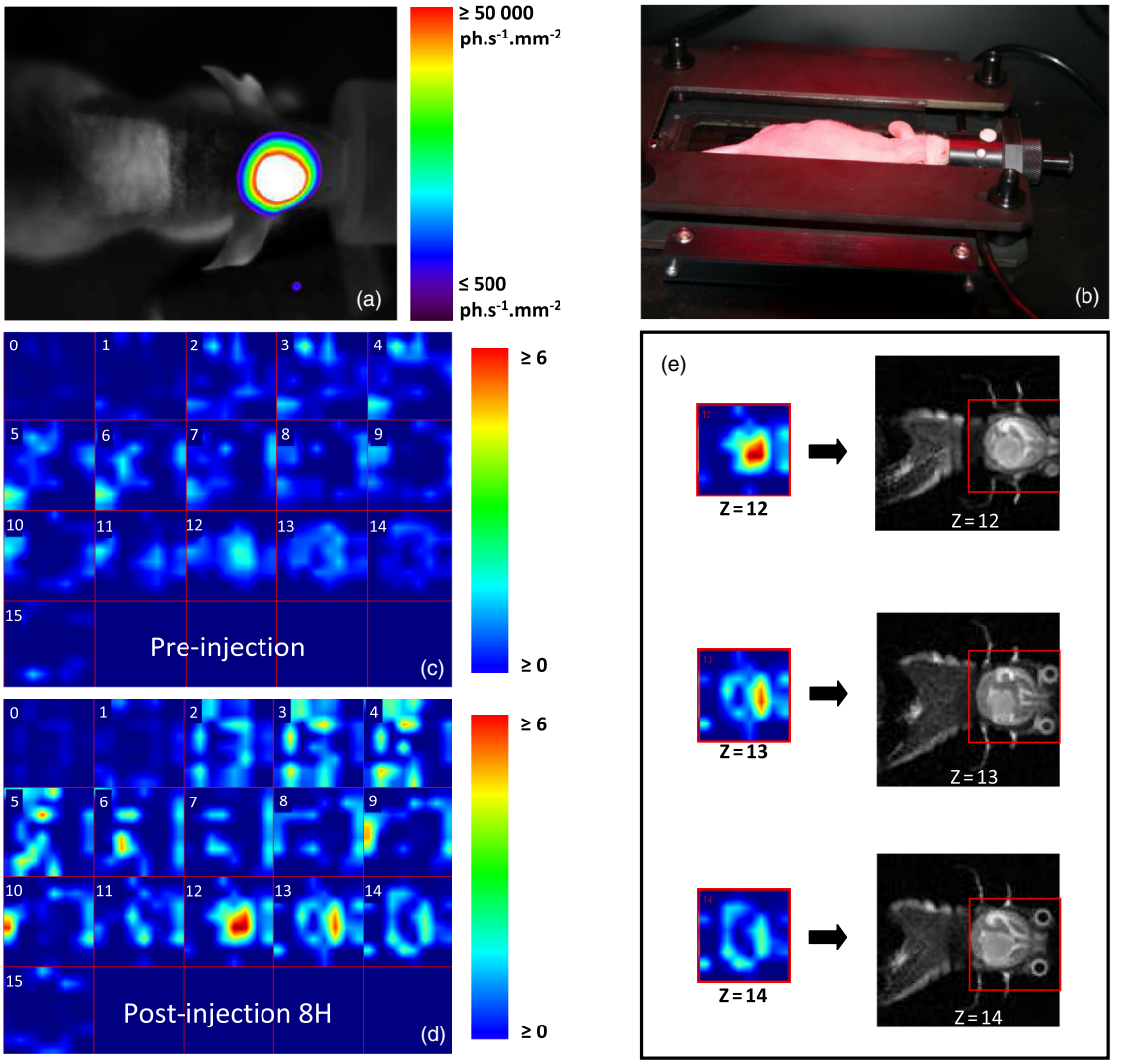

Fig. 2 Imaging of a brain tumor. (a) Bioluminescence image of a mouse bearing an intracerebral U87-CMV-lucF tumor. (b) Picture of the mouse in the fDOT double-plate contention holder. Upper glass plate is limited to the mouse's head. (c) and (d) Results of fDOT reconstructions before (c) and 8 h (d) after DiR-lipidots injection. Z cross-sections (1 mm thickness) are presented in the same color scale from $z = 0$ (ventral) to $z = 15$ (dorsal). (e): T2-weighted MR images of the same mouse maintained in the fDOT double-plate contention holder. $Z = 12$ to $z = 14$ cross-sections (1 mm thickness corresponding with the fDOT frame) showing the brain tumor localization. Slices ($z = 0$ to $z = 9$) corresponding with the outside of the brain. Images are representative of $n =$ six mice.

Mice used for multi-imaging sequence exhibited a BLI signal from the brain tumor above 200,000 photons $\cdot$ s^{-1} $\cdot$ mm^{-2}. Mice were first imaged by BLI [Fig. 2(a)] and immediately submitted to a fDOT acquisition [Fig. 2(c)]. The 3-D fluorescent maps computed using the fDOT software provide a stack of 16 fluorescent slices with 1 mm of thickness, from ventral ($z = 0$) to dorsal ($z = 15$). As shown in Fig. 2(c) substantial amounts of fluorescence were detected before DiR-lipidots injection. After a fDOT acquisition, mice are allowed to rescue from anesthesia (10 min) and are then injected intravenously with the DiR-lipidots solution. MRI and fDOT were performed 8 h after injection, sequentially and using the double plates contention support [Fig. 2(b)].

As shown on Fig. 2(d), the 3-D fluorescent maps reveal fluorescent hot spots on slices $z = 12$, $z = 13$, and $z = 14$. The MRI images are fitted on the fDOT thickness to provide the same stack of slices (1 mm of thickness). fDOT and MRI images from the z-stack were compared z-slice to z-slice. As shown in Fig. 2(e), slices $z = 12$, $z = 13$, and $z = 14$ exhibiting hot fluorescent spots fit with MRI slices corresponding to brain tumors location. A substantial amount of fluorescent signal was also found outside the brain in slices ($z = 0$ to $z = 9$) corresponding to the buccal area. Alternatively, fluorescence distribution of the DiR dye could be provided as a 3-D representation as illustrated in Fig. 3.

4 Discussion

Fluorescence tomography is a cost-effective method for tumor detection and localization in preclinical models.[1,13] Improved imaging systems and a growing number of fluorescent agents are now commercially available. Most of fluorescent probes are designed for molecular imaging purpose [i.e., they are targeted or activatable to reveal some molecular characteristic of the tissues related to the malignant status (see Molecular Imaging and Contrast Agent Database (MICAD) at NCBI)]. Accumulation of nanoparticles from the blood stream into the

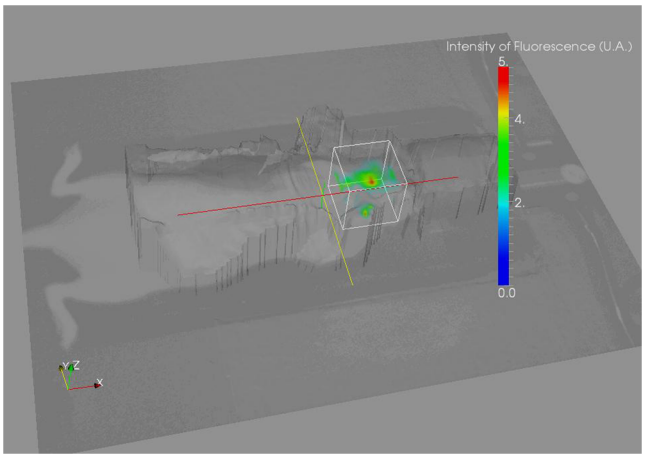

Fig. 3 3-D imaging of fDOT reconstruction after DiR-lipidots injection of a mouse bearing an intracerebral U87-CMV-lucF tumor. Image representative of the same batch of animals than Fig. 2 ($n = 6$).

tumor is essentially due to the EPR phenomena, a complex biological process that remains variable and unpredictable regarding to the level of particles accumulation and their distribution within the tumor micro-environment.[14,15] It is linked to the defects of the vascular wall that promote the extravasation of particles from the blood pool, and the low lymphatic drainage that limits their elimination from the tumor area.[7,15]

Despite some uncontrolled aspect, the EPR phenomenon remains the major process used to gain imaging contrast in tumors from circulating blood pool agents.[14] Our present goal was to show that such a nonspecific blood pool agent, namely DiR-loaded lipid nanoparticles, could be used in combination with fluorescence tomography to detect deep tumors using the EPR effect without any prerequisite knowledge on the tumor molecular signature.

Systemic injection of the DiR-loaded lipid nanoparticles results in a rapid increase of the fluorescent signal in all tissues of mice. The fluorescent level peaks about 8 h after injection then decreases rapidly during the next 15 h. The fluorescence level in the tumor is higher than in surrounding tissues and decreases more slowly probably due to the EPR phenomenon and provides the opportunity to use DiR-lipidots as contrast agent for imaging. In subcutaneous tumor, substantial amount of fluorescence remains detectable up to seven days after injection.

fDOT provided 3-D fluorescent maps allowing for a localization of subcutaneous tumor consistent with the MRI observation. The free space mode acquisition system was used because it is difficult to place subcutaneous tumor on a mouse's leg in contact with the double-glass plate system. Fluorescence maps clearly localize the tumor at the top of the leg level with almost no auto-fluorescence signal (pre-injection fluorescence maps) and limited fluorescence artifact outside the tumor.

fDOT 3-D fluorescence maps for brain tumor were obtained using the double-plate acquisition system. Indeed, using the free space acquisition system, the orientation of the scanning laser (45°) results in a shadow behind the skull that impacts the 3-D reconstruction. The calculated fDOT localization is consistent with tumor localization determined by MRI. Fluorescent hot spots on 3-D fluorescence maps were found for the same slices than tumor contrast by recorded MRI. It is important to note that MRI resolution has been reduced to fit with the fluorescence 3-D maps providing a 1-mm resolution in the z axis. fDOT fluorescence maps also reveal fluorescent hot spots outside the brain. These spots are not related to disseminated U87 cells or metastases because no BLI signal was detected outside the brain. Some of these correspond to auto-fluorescence signals already noted before injection, but others clearly appear after DiR-lipidots injection and could be due to changes of vascular permeability outside the tumor, as in lymph nodes.[16] Dye-loaded lipidots have previously been demonstrated to be efficient contrast agents for the lymphatic system and lymph nodes.[10] Alternatively, fluorescent spots may also result from unspecific binding of nanoparticles.

The presence of auto-fluorescent spots outside the tumor remains the major limitation for the current strategy. Near-infrared (NiR) fluorescence (650 to 900 nm) detection was believed to limit the natural background fluorescence of living tissues.[1,17,18] Our study shows that it is the case in the legs and brains of mice as demonstrated by the 3-D fluorescent maps obtained before injection. However, some auto-fluorescence was clearly detected in mice heads outside the brain. In the abdominal cavity, spontaneous fluorescence from tissues such as stomach, liver, and gut appeared critical and impaired fDOT tumor detection with DiR-lipidots (data not shown). An alfalfa-free diet was reported to reduce tissue auto-fluorescence[19] but, in our experience, it didn't change the level of pre-injection signal visible on the head outside the brain.

In the present work, BLI is clearly the most sensitive imaging modality for tumor detection. The BLI signal of the U87-CMV-lucF cells could be detected at any time after cells injection suggesting that luciferin freely reached U87 cells. Because BLI signal only results from lucF expression and activity, this imaging modality is restrained to the detection of genetically modified cells. Tumor detection using fDOT occurs later when tumors reach a significant size (i.e., with a large number of tumor cells). We have not yet determined if the limit of detection using the fDOT/DiR-lipidots methodology is due to the sensitivity of the imaging method or linked to an insufficient EPR effect. The EPR effect only occurred after the angiogenic switch[7] and is crucial for accumulation of the DiR-lipidots (35 nm diameter) within the tumor environment.

5 Conclusions

Nanotechnologies have provided a great expectation for cancer detection, prevention, and treatment. Nanoparticles allow for loading high concentrations of different types of chemicals, providing a way to link the fate of the therapeutic agent to the fate of the imaging agent. fDOT appears to be a cost-effective, safe, and valuable technique to study nanoparticle distribution within animal tissues. Due to the EPR phenomena, nontargeted nanoparticles accumulate in tumor environment and could be used to localize tumors within tissues such as muscles or brain, exhibiting low fluorescence complexity. However, further improvements are still required at the level of both imaging systems and nanoparticles, to increase the imaging contrast and to better discriminate tumor labeling from surrounding tissues in more complex optical environments, such as the abdominal cavity.

Acknowledgments

The authors would like to thank Dr. Bruno Quesson and Dr. Matthieu Lepetit-Coiffé for assistance in MRI, Dr. Nora Frulio for valuable discussion and Professor Nicolas Grenier for critical reading of the manuscript. This work was supported

by Agence Nationale pour la Recherche ANR-RNTS: Tomofluo3D and Ligue contre le Cancer.

References

1. R. Weissleder and M. J. Pittet, "Imaging in the era of molecular oncology," *Nature* **452**(7187), 580–589 (2008).
2. R. Weissleder and V. Ntziachristos, "Shedding light onto live molecular targets," *Nat. Med.* **9**(1), 123–128 (2003).
3. V. Ntziachristos et al., "Fluorescence molecular tomography resolves protease activity *in vivo*," *Nat. Med.* **8**(7), 757–760 (2002).
4. M. A. O'Leary et al., "Fluorescence lifetime imaging in turbid media," *Opt. Lett.* **21**(2), 158–160 (1996).
5. A. Garofalakis et al., "*In vivo* validation of free-space fluorescence tomography using nuclear imaging," *Opt. Lett.* **35**(18), 3024–3026 (2010).
6. A. Koenig et al., "*In vivo* mice lung tumor follow-up with fluorescence diffuse optical tomography," *J. Biomed. Opt.* **13**(1), 011008 (2008).
7. H. Maeda et al., "Tumor vascular permeability and the EPR effect in macromolecular therapeutics: a review," *J. Control Release* **65**(1–2), 271–284 (2000).
8. M. Goutayer et al., "Tumor targeting of functionalized lipid nanoparticles: assessment by *in vivo* fluorescence imaging," *Eur. J. Pharm. Biopharm.* **75**(2), 137–147 (2010).
9. I. Texier et al., "Cyanine-loaded lipid nanoparticles for improved *in vivo* fluorescence imaging," *J. Biomed. Opt.* **14**(5), 054005 (2009).
10. J. Gravier et al., "Lipidots: competitive organic alternative to quantum dots for *in vivo* fluorescence imaging," *J. Biomed. Opt.* **16**(9), 096013 (2011).
11. A. Koenig et al., "Fluorescence diffuse optical tomography for free-space and multifluorophore studies," *J. Biomed. Opt.* **15**(1), 016016 (2010).
12. L. Hervé et al., "Noncontact fluorescence diffuse optical tomography of heterogeneous media," *Appl. Opt.* **46**(22), 4896–4906 (2007).
13. V. Ntziachristos et al., "Visualization of antitumor treatment by means of fluorescence molecular tomography with an annexin V-Cy5.5 conjugate," *Proc. Natl. Acad. Sci. U. S. A.* **101**(33), 12294–12299 (2004).
14. R. K. Jain and T. Stylianopoulos, "Delivering nanomedicine to solid tumors," *Nat. Rev. Clin. Oncol.* **7**(11), 653–664 (2010).
15. V. Torchilin, "Tumor delivery of macromolecular drugs based on the EPR effect," *Adv. Drug Deliv. Rev.* **63**(3), 131–135 (2011).
16. R. Jain, P. Dandekar, and V. Patravale, "Diagnostic nanocarriers for sentinel lymph node imaging," *J. Control Release* **138**(2), 90–102 (2009).
17. V. Ntziachristos, C. Bremer, and R. Weissleder, "Fluorescence imaging with near-infrared light: new technological advances that enable in vivo molecular imaging," *Eur. Radiol.* **13**(1), 195–208 (2003).
18. B. Ballou, L. A. Ernst, and A. S. Waggoner, "Fluorescence imaging of tumors *in vivo*," *Curr. Med. Chem.* **12**(7), 795–805 (2005).
19. Y. Inoue et al., "Diet and abdominal autofluorescence detected by *in vivo* fluorescence imaging of living mice," *Mol. Imaging* **7**(1), 21–27 (2008).